13th International Symposium on Turbulence and Shear Flow Phenomena (TSFP13)
Montreal, Canada, June 25–28, 2024

ESTIMATING MEAN PROFILES AND FLUXES IN HIGH-SPEED TURBULENT BOUNDARY LAYERS USING INNER/OUTER-LAYER TRANSFORMATIONS

Asif Manzoor Hasan
Process and Energy Department
Delft University of Technology
Leeghwaterstraat 39, 2628 CB, Delft, The Netherlands
a.m.hasan@tudelft.nl

Johan Larsson
Department of Mechanical Engineering
University of Maryland
College Park, MD 20742, USA
jola@umd.edu

Sergio Pirozzoli
DIMA
Sapienza Università di Roma
Via Eudossiana 18, 00184 Roma, Italy
sergio.pirozzoli@uniroma1.it

Rene Pecnik
Process and Energy Department
Delft University of Technology
Leeghwaterstraat 39, 2628 CB, Delft, The Netherlands
r.pecnik@tudelft.nl

Introduction

Accurately predicting drag and heat transfer for compressible high-speed flows is of utmost importance for a range of engineering applications. A common approach is to use compressible velocity scaling laws (transformation), that inverse transform the velocity profile of an incompressible flow, together with a temperature-velocity relation. Current methods (Huang *et al.*, 1993; Kumar & Larsson, 2022) typically assume a single velocity scaling law, neglecting the different scaling characteristics of the inner and outer layers. Here, we use distinct velocity transformations for these two regions. In the inner layer, we utilize a recently proposed scaling law that appropriately incorporates variable property and intrinsic compressibility effects (Hasan *et al.*, 2023), while the outer layer profile is inverse-transformed with the well-known Van Driest transformation (Van Driest, 1951). The result is an analytical expression for the mean shear valid in the entire boundary layer, which combined with the temperature-velocity relationship in Zhang *et al.* (2014), provides predictions of mean velocity and temperature profiles at high accuracy. Using these profiles, drag and heat transfer is evaluated with an accuracy of +/-4% and +/-8%, respectively, for a wide range of compressible turbulent boundary layers up to Mach numbers of 14.

Proposed Method

An incompressible velocity profile is composed of two parts: (1) the law of the wall in the inner layer, and (2) the velocity defect law in the outer layer. We can model the law of the wall either by composite velocity profiles (Musker, 1979; Chauhan *et al.*, 2007; Nagib & Chauhan, 2008), or by integrating the mean momentum equation using a suitable eddy viscosity model (Van Driest, 1956*a*; Johnson & King, 1985). Here, we follow the latter approach and utilize the Johnson-King (Johnson & King, 1985) eddy viscosity model. Likewise, there are several formulations available to represent the defect law (Coles, 1956; Zagarola & Smits, 1998; Fernholz & Finley, 1996), of which we use Coles' law of the wake (Coles, 1956).

Once the reference incompressible velocity profile is obtained, we inverse transform it using our recently proposed velocity transformation (Hasan *et al.*, 2023) for the inner layer, and the Van Driest (VD) transformation (Van Driest, 1951) for the outer layer. They are combined as follows:

$$d\bar{u}^+ = f_3^{-1} f_2^{-1} f_1^{-1} d\bar{U}^+_{inner} + f_1^{-1} d\bar{U}^+_{wake} \tag{1}$$

where the factors f_1, f_2, and f_3 constitute the transformation kernel proposed in Hasan *et al.* (2023) that accounts for both variable property and intrinsic compressibility effects, given as

$$\frac{d\bar{U}^+}{d\bar{u}^+} = \underbrace{\left(\frac{1+\kappa y^* D(y^*,M_\tau)}{1+\kappa y^* D(y^*,0)}\right)}_{f_3} \underbrace{\left(1-\frac{y}{\delta_v^*}\frac{d\delta_v^*}{dy}\right)}_{f_2} \underbrace{\sqrt{\frac{\bar{\rho}}{\rho_w}}}_{f_1} \tag{2}$$

$$D(y^*,M_\tau) = \left[1-\exp\left(\frac{-y^*}{A^+ + f(M_\tau)}\right)\right]^2 \tag{3}$$

The value of A^+ differs based on the choice of the von Kármán constant κ, such that the log-law intercept is reproduced for that κ (Nagib & Chauhan, 2008). With $\kappa = 0.41$, the value of $A^+ = 17$ gives a log-law intercept of 5.2 (Iyer & Malik, 2019), whereas, with $\kappa = 0.384$, $A^+ = 15.22$ gives a log-law intercept of 4.17. The additive term $f(M_\tau)$ accounts for intrinsic compressibility effects. Hasan *et al.* (2023) proposed $f(M_\tau) = 19.3M_\tau$, that is independent of the chosen value of κ.

In the equations above, $\bar{u}$ and $\bar{U}$ represent mean velocity for compressible and incompressible flows, respectively. $y^* = y/\delta_v^*$ is the semi-local wall-normal coordinate where $\delta_v^* = \bar{\mu}/(\bar{\rho}u_\tau^*)$ is the semi-local viscous length scale, $u_\tau^* = \sqrt{\tau_w/\bar{\rho}}$ is the semi-local friction velocity scale, and $\bar{\rho}$ and $\bar{\mu}$ represent mean density and dynamic viscosity, respectively. $M_\tau = u_\tau/a_w$ is the friction Mach number, where u_τ and a_w

are friction velocity and sound speed defined at the wall, respectively. Superscript '+' implies wall-scaling, subscript 'w' implies value at the wall, and $\overline{(.)}$ denotes Reynolds averaging.

In Eq. (1), $d\bar{U}^+_{inner}$ is modeled using the Johnson-King eddy viscosity model as $dy^*/[1+\kappa y^* D(y^*,0)]$, and $d\bar{U}^+_{wake} = \Pi/\kappa \sin(\pi y/\delta)\,\pi\, d(y/\delta)$ is the derivative of the Coles' wake function. Here, Π represents the wake parameter and δ ($=\delta_{99}$) is the boundary layer thickness. Inserting the expressions for $d\bar{U}^+_{inner}, d\bar{U}^+_{wake}$ in Eq. (1), using $dy^*/dy = f_2/\delta^*_v$, $u^*_\tau = u_\tau f_1^{-1}$, and upon rearrangement, we get the dimensional form of the mean velocity gradient as

$$\frac{d\bar{u}}{dy} = \frac{u^*_\tau}{\delta^*_v}\frac{1}{1+\kappa y^* D(y^*,M_\tau)} + \frac{u^*_\tau}{\delta}\frac{\Pi}{\kappa}\pi \sin\left(\pi\frac{y}{\delta}\right) \quad (4)$$

Eq. (4) provides several useful insights. Analogous to an incompressible flow, the mean velocity in a compressible flow is controlled by two distinct length scales, δ^*_v and δ, characteristic of the inner and outer layers, respectively. The two layers are connected by a common velocity scale u^*_τ (the semi-local friction velocity), leading to a logarithmic law in the overlap region. Moreover, in the logarithmic layer and beyond, the first term on the right hand side reduces to $\sqrt{\tau_w/\bar{\rho}}/(\kappa y)$, which is consistent with Van Driest's original arguments (Van Driest, 1951). It is crucial to satisfy this condition; otherwise, the logarithmic profile extending to the outer layer would not obey Van Driest's scaling, while the wake component to which it is added would. The compressibility transformation used in this paper (Hasan *et al.*, 2023) naturally satisfies this condition, however, other transformations like the ones in Volpiani *et al.* (2020) and Griffin *et al.* (2021) don't. To address this issue Van Driest's scaling is enforced in the outer layer for these transformations as discussed in Appendix A.

For convenience, Eq. (4) can also be expressed in terms of the dimensional variables τ_w, $\bar{\mu}$ and $\bar{\rho}$ as,

$$\frac{d\bar{u}}{dy} = \frac{\tau_w}{\bar{\mu} + \underbrace{\sqrt{\tau_w\bar{\rho}}\,\kappa y D(y^*,M_\tau)}_{\mu_t}} + \frac{\sqrt{\tau_w/\bar{\rho}}}{\delta}\frac{\Pi}{\kappa}\pi\sin\left(\pi\frac{y}{\delta}\right) \quad (5)$$

where μ_t is the Johnson-King eddy viscosity model corrected for intrinsic compressibility effects, as after the transformation of Hasan *et al.* (2023). It can be readily used in turbulence modeling, for instance, as a wall-model in large eddy simulations.

The second term on the right-hand-side of Eq. (5) is the wake term accounting for mean density variations, where Coles' wake parameter Π depends on the Reynolds number[1], as discussed in the subsection below.

Characterizing low-Reynolds-number effects on the wake parameter

For incompressible boundary layers, Coles' wake parameter is known to strongly depend on Re_θ (free-stream Reynolds number defined as $\rho_\infty u_\infty \theta/\mu_\infty$, where θ is the momentum thickeness and subscript '∞' represents free-stream conditions) at low Reynolds numbers (Coles, 1962; Fernholz & Finley, 1996; Cebeci & Smith, 1974). For compressible boundary layers, the ambiguity of the optimal Reynolds number definition poses a challenge to characterize the wake parameter. Fernholz & Finley (1980), mainly using experimental data at that time, observed that the momentum-thickness Reynolds number with viscosity at the wall ($Re_{\delta_2} = \rho_\infty u_\infty \theta/\mu_w$) is the suitable definition to scale Π. On the other hand, Wenzel *et al.* (2018) observed that the wake parameter scales with Re_θ for their direct numerical simulations (DNS) at moderate free-stream Mach numbers ($M_\infty \leq 2.5$), consistent with the expectation that Π (being defined at the boundary layer edge) should scale with Reynolds number based on the free-stream properties (Smits & Dussauge, 2006; Cebeci & Smith, 1974). Yet, there is no clear consensus on which definition is relevant in scaling Π, especially for high-Mach-number flows where Re_{δ_2} and Re_θ are quite different from each other. Given the recent availability of hypersonic DNS database, we revisit the question of which Reynolds number best describes the wake parameter.

First, we evaluate Π for several incompressible and compressible DNS cases from the literature and then report it as a function of different definitions of the Reynolds number, searching for the definition yielding the least spread of the data points. For incompressible flows, the wake strength can be determined as $\Pi = 0.5\kappa\left(\bar{U}^+(y=\delta) - 1/\kappa\ln(\delta^+) - C\right)$, where C is the log-law intercept for the chosen κ. For compressible flows, the wake strength is based on the VD transformed velocity (Fernholz & Finley, 1980; Smits & Dussauge, 2006) as $\Pi = 0.5\kappa\left(\bar{U}^+_{vd}(y=\delta) - (\bar{U}^+_{vd})^{log}(y=\delta)\right)$, where $\bar{U}^+_{vd}$ is obtained from the DNS data. The reference log law $(\bar{U}^+_{vd})^{log}$, unlike for incompressible flows, cannot be computed as $1/\kappa\ln(y^+)+C_{vd}$, because C_{vd} is found to be non-universal for diabatic compressible boundary layers (Bradshaw, 1977; Trettel & Larsson, 2016). Hence, $(\bar{U}^+_{vd})^{log}$ can be obtained either by fitting a logarithmic curve to $\bar{U}^+_{vd}$ (Fernholz & Finley, 1980), or by inverse transforming the incompressible law of the wall. Here, we follow the latter approach by using the compressibility transformation of Hasan *et al.* (2023).

The value of the von Kármán constant κ plays a crucial role in estimating Π. Spalart (1988) noted that a strong consensus on κ is needed to accurately estimate Π. However, such a consensus is yet missing (Monkewitz & Nagib, 2023). Nagib & Chauhan (2008) showed that $\kappa = 0.384$ is a suitable choice for incompressible boundary layers, verified to be true also for channels (Lee & Moser, 2015) and pipes (Pirozzoli *et al.*, 2021). However, due to historical reasons and wide acceptance of $\kappa = 0.41$, we will proceed with this value. The same procedure can straightforwardly be repeated with a different value of κ.

Figure 1 shows the wake parameter for twenty-six compressible and nineteen incompressible boundary layer flows, as a function of Re_{δ_2}, Re_θ (defined above), $Re_{\delta^*} = \rho_\infty u_\infty \delta^*/\mu_\infty$ (where δ^* is the displacement thickness) and $Re^*_{\tau_\infty} = \rho_\infty u^*_{\tau_\infty}\delta/\mu_\infty$ (the semi-local Reynolds number defined using free-stream properties). The spread in the data points is found to be quite large for all the definitions, as Π is the difference of two relatively large quantities, namely $\bar{U}^+_{vd}$ and $(\bar{U}^+_{vd})^{log}$ at the boundary layer edge, as outlined above. Note that even incompressible boundary layers are not devoid of this scatter (Spalart, 1988; Fernholz & Finley, 1996). Figure 1(a) shows the presence of two distinct branches, hence Re_{δ_2} does not seem to be suitable to characterize Π, unlike reported in previous literature (Fernholz & Finley, 1980; Huang *et al.*, 1993). Among the four definitions of Reynolds number, Re_θ seems to show the least spread, further confirming the conclusion in Wenzel *et al.* (2018). Figure 1(b) also reports several

[1]The wake parameter also depends on pressure gradient (Coles, 1956), however, the focus here is limited to zero pressure gradient turbulent boundary layers

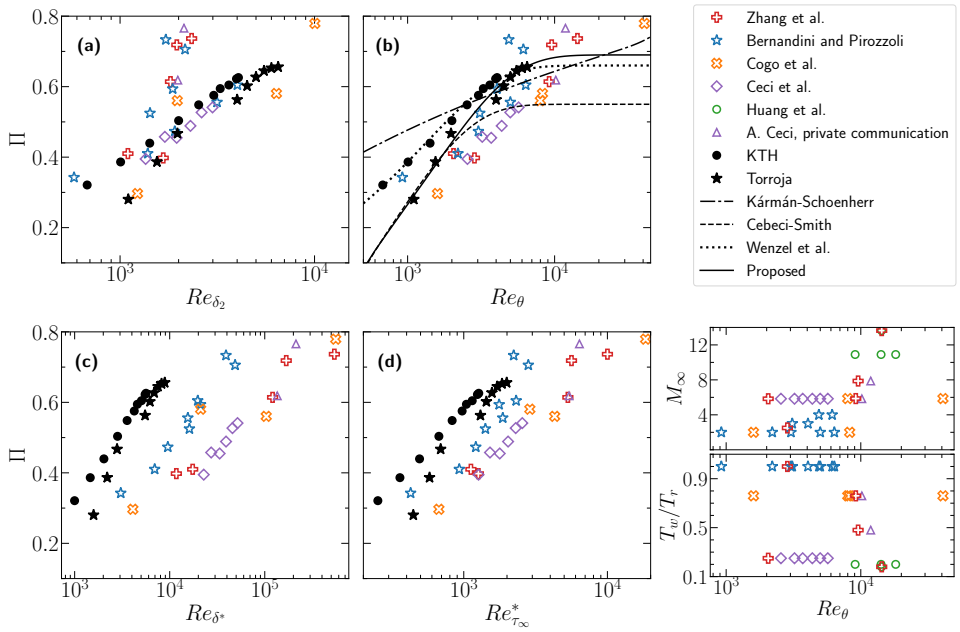

Figure 1. The wake parameter Π computed using the DNS data and plotted as a function of (a) Re_{δ_2} (b) Re_θ (c) Re_{δ^*} and (d) $Re^*_{\tau_\infty}$ for 19 incompressible (Schlatter *et al.*, 2009; Schlatter & Örlü, 2010; Jiménez *et al.*, 2010; Sillero *et al.*, 2013) and 26 compressible (Zhang *et al.*, 2018; Bernardini & Pirozzoli, 2011; Cogo *et al.*, 2022; Ceci *et al.*, 2022, A. Ceci, private communication) turbulent boundary layers. M_∞ is the free-stream Mach number and T_w/T_r is the ratio of wall and recovery temperatures.

functional forms of $\Pi = f(Re_\theta)$. Use of the modified Kármán-Schoenherr friction formula (Nagib *et al.*, 2007) for indirect evaluation of Π does not show saturation at high Reynolds numbers[2]. The Cebeci-Smith (hereby CS) relation (Cebeci & Smith, 1974) underpredicts Π, but reproduces saturation at high Reynolds numbers. Wenzel *et al.* (2018) modified the CS relation with a higher saturation value of Π (0.66) and made it to fit the DNS data of Schlatter *et al.* (2009) and Schlatter & Örlü (2010). Here, we propose a relation similar to that proposed by (Cebeci & Smith, 1974), to achieve a better fit with data from more recent incompressible DNS of Jiménez *et al.* (2010) and Sillero *et al.* (2013). The relation is

$$\Pi = 0.69\left[1 - \exp(-0.243\sqrt{z} - 0.15z)\right] \tag{6}$$

where $z = Re_\theta/425 - 1$. The proposed curve collapses with the CS relation at low Reynolds numbers and differs from it mainly in the high-Reynolds-number saturated region.

Implementation

Eq. (5) covers the entire boundary layer, and it can be integrated in conjunction with a suitable temperature model such as the one proposed by Zhang *et al.* (2014), which is given as

$$\frac{\bar{T}}{T_w} = 1 + \frac{T_r - T_w}{T_w}\left[(1 - sPr)\left(\frac{\bar{u}}{u_\infty}\right)^2 + sPr\left(\frac{\bar{u}}{u_\infty}\right)\right] + \frac{T_\infty - T_r}{T_w}\left(\frac{\bar{u}}{u_\infty}\right)^2 \tag{7}$$

where $sPr = 0.8$, $T_r/T_\infty = 1 + 0.5r(\gamma - 1)M_\infty^2$, $r = Pr^{1/3}$, with T_w, T_∞ and T_r being the wall, free-stream and recovery temperatures, respectively, and Pr being the Prandtl number. Moreover, a suitable viscosity law (e.g., power or Sutherland's law), and the ideal gas equation of state $\bar{\rho}/\rho_w = T_w/\bar{T}$ have to be used to compute mean viscosity and density profiles, respectively. The inputs that need to be provided are the Reynolds number (Re_θ), free-stream Mach number (M_∞), wall cooling/heating parameter (T_w/T_r) and (optionally) the dimensional wall or free-stream temperature for Sutherland's law. It is important to note that Eq. (7), and all solver inputs are based on the quantities in the free-stream, and not at the boundary layer edge ($y = \delta_{99}$). For more insights, refer to the source code available on GitHub (Pecnik & Hasan, 2023).

Results

Figure 2 shows the predicted velocity and temperature profiles for a selection of high Mach number cases. As can be seen, the DNS and the predicted profiles are in good agreement, thus corroborating our methodology. The insets in Figure 2 show the error in the predicted skin-friction ($c_f = 2\tau_w/[\rho_\infty u_\infty^2]$) and heat-transfer ($c_h = q_w/[c_p\rho_\infty u_\infty(T_w - T_r)]$) coefficients for thirty compressible cases from the literature. For most cases, the friction coefficient is predicted with $+/-$ 4% accuracy, with a maximum error of -5.3%. The prediction of the heat-transfer coefficient shows a slightly larger error compared to c_f, potentially due to additional inaccuracies arising from the temperature-velocity relation. In most cases, c_h is predicted with $+/-8\%$ accuracy, with a maximum error of 10.3%.

In order to check the sensitivity of the predictions to the relation used for the wake parameter, we recomputed the results using our method but instead of using Eq. (6) to estimate Π, we employed the relation proposed in Wenzel *et al.* (2018). The maximum error in the c_f prediction changed from -5.3% to -6.08%, with most of the cases within error bounds of $+/-5\%$. For c_h prediction, there was an increase in the maximum error from 10.3% to 11.4%, with most of the cases

[2]Saturation at high Reynolds numbers was observed in Coles (1962) for incompressible boundary layers.

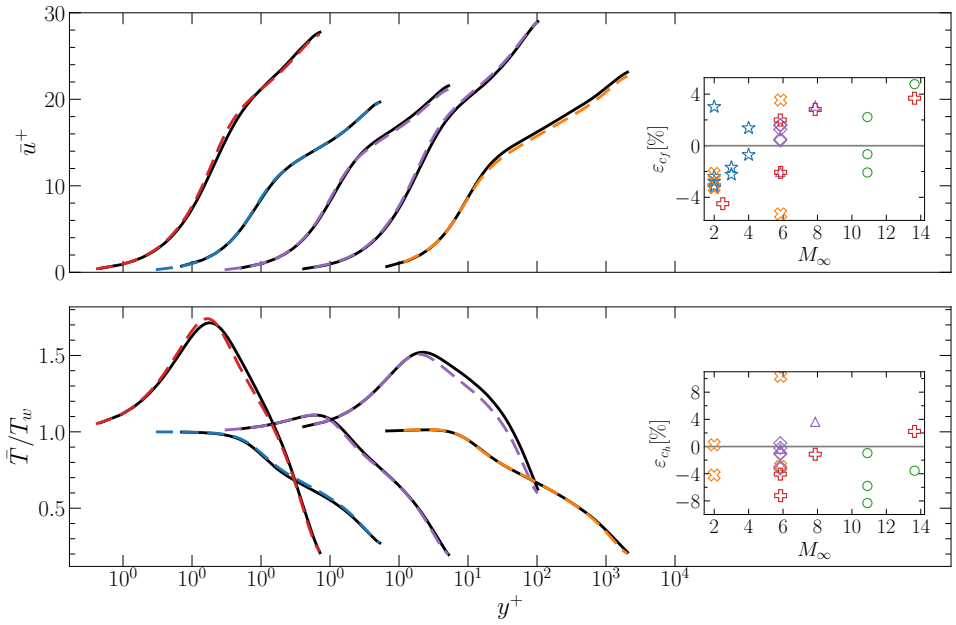

Figure 2. Predicted velocity (top) and temperature (bottom) profiles (dashed lines) compared to DNS (black solid lines) for the cases with the highest reported Mach numbers in the respective publications: (left to right) $M_\infty = 13.64$, $T_w/T_r = 0.18$ (Zhang *et al.*, 2018); $M_\infty = 4$, $T_w/T_r = 1$ (Bernardini & Pirozzoli, 2011); $M_\infty = 7.87$, $T_w/T_r = 0.48$ (A. Ceci, private communication); $M_\infty = 5.84$, $T_w/T_r = 0.25$ (Ceci *et al.*, 2022); $M_\infty = 5.86$, $T_w/T_r = 0.76$ (Cogo *et al.*, 2022). (Insets): Percent error in skin-friction (top) and heat-transfer (bottom) prediction for 30 compressible turbulent boundary layers from the literature (Bernardini & Pirozzoli, 2011; Zhang *et al.*, 2018; Ceci *et al.*, 2022; Cogo *et al.*, 2022; Huang *et al.*, 2020, A. Ceci, private communication). The error is computed as $\varepsilon_{c_f} = (c_f - c_f^{DNS})/c_f^{DNS} \times 100$ and likewise for ε_{c_h}. Symbols are as in Figure 1.

within error bounds of $+/-8\%$.

The proposed method is modular in that it can also be applied using other inner-layer transformations (Griffin *et al.*, 2021; Volpiani *et al.*, 2020; Trettel & Larsson, 2016; Patel *et al.*, 2016) with minor modifications as discussed in Appendix A. This is shown in Figure 3, which compares the proposed approach with another modular approach of Kumar & Larsson (2022), both with different inner layer transformations. Additionally, the figure includes results obtained with the method of Huang *et al.* (1993) using the VD transformation, and the widely recognized Van Driest II skin-friction formula (Van Driest, 1956*b*). Figure 3 also shows the root-mean-square error, determined as RMS $= \sqrt{1/N \sum \varepsilon_{c_f}^2}$, where N is the total number of DNS cases considered. The Van Driest II formula and the method of Huang *et al.* have similar RMS error of about 6% [3], which is not surprising as both of them are built on Van Driest's mixing-length arguments. The errors are selectively positive for majority of the cases, and it increases with higher Mach number and stronger wall cooling. The source of this error mainly resides in the inaccuracy of the VD velocity transformation in the near-wall region for diabatic flows. To eliminate this shortcoming, Kumar & Larsson (2022) developed a modular methodology, which is quite accurate when the transformation of Volpiani *et al.* (2020) is used, but it is less accurate if other velocity transformations are implemented. This inaccuracy is because the outer layer velocity profile is also inverse-transformed according to the inner-layer transformation. In the current approach, the velocity profile is instead inverse-transformed using two distinct transformations, which take into account the different scaling properties of the inner and outer layers, thus reducing the RMS error with respect to Kumar and Larsson's modular method for all the transformations tested herein. The error using the proposed approach with the TL transformation is preferentially positive for all the cases. This is due to the log-law shift observed in the TL scaling, which is effectively removed in the Hasan *et al.* transformation, thereby yielding an RMS error of 2.66%, which is the lowest among all approaches.

Conclusion

We have derived an expression for the mean velocity gradient in high-speed boundary layers [Eq. (5)] that combines the inner-layer transformation recently proposed by Hasan *et al.* (2023) and the Van Driest (1951) outer-layer transformation, thus covering the entire boundary layer. The Coles' wake parameter in this expression is determined using an adjusted Cebeci and Smith relation [Eq. (6)] with the definition of Re_θ as the most suitable parameter to characterize low-Reynolds-number effects on Π. This method allows remarkably accurate predictions of the mean velocity and temperature profiles, leading to estimation of the friction and heat-transfer coefficients which are within $+/-4\%$ and $+/-8\%$ error bounds with respect to DNS data, respectively. When compared with other skin-friction prediction methods in literature, our approach yields the lowest RMS error of 2.66%.

The methodology developed in this paper promises straightforward application to other classes of wall-bounded flows like channels and pipes, upon change of the temperature-velocity relation (e.g. Song *et al.*, 2022), and using different values of the wake parameter Π (Nagib & Chauhan, 2008). Also, the method is modular in the sense that it can be used with other temperature models and equations of state, and can

[3] Huang *et al.*'s method with the more accurate temperature velocity relation in Zhang *et al.* (2014) leads to an RMS error of 12%.

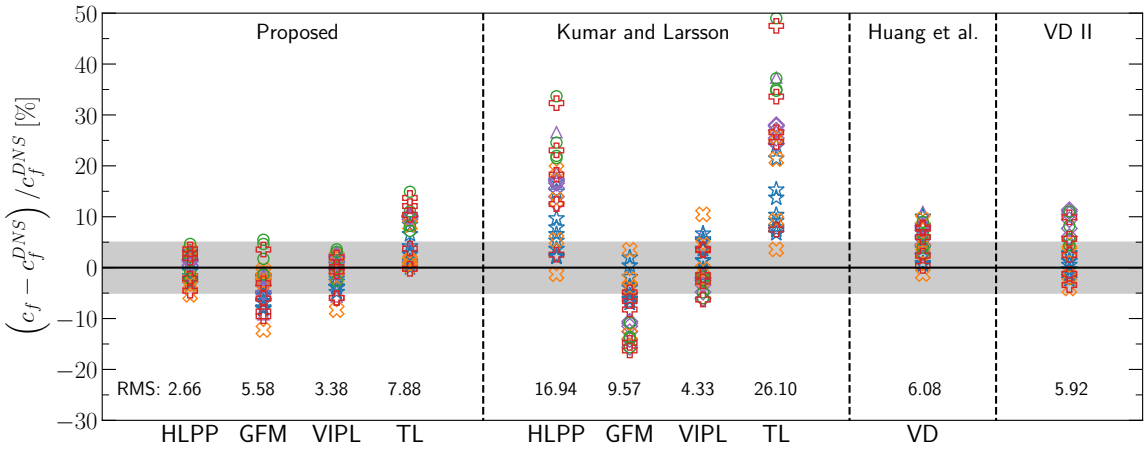

Figure 3. Error in skin-friction prediction using the proposed approach compared to different state-of-the-art approaches. The letters on the X-axis denote the velocity transformation used for that approach. HLPP, GFM, VIPL, TL, and VD stand for the transformations proposed in Hasan *et al.* (2023), Griffin *et al.* (2021), Volpiani *et al.* (2020), Trettel & Larsson (2016), and Van Driest (1951), respectively. The numbers are RMS values computed as outlined in the text. Symbols are as in Figure 1. The shaded region shows an error bar of +/-5%. Note that inputs for all the methods are based on properties in the free-stream instead of at the edge of the boundary layer.

also be extended to non-equilibrium boundary layers with appropriate modifications.

Appendix A: Implementation of the method using velocity transformations in Ref. (Griffin *et al.*, 2021; Volpiani *et al.*, 2020)

As outlined earlier, in the logarithmic region and beyond, the first term on the right-hand side of Eq. (5) reduces to $\sqrt{\tau_w/\bar{\rho}}/(\kappa y)$, which is the same as Van Driest's original arguments (Van Driest, 1951). It is crucial to satisfy this condition, otherwise the logarithmic profile extending to the outer layer would not obey Van Driest's scaling. The transformations of Griffin *et al.* (2021); Volpiani *et al.* (2020) fail to satisfy this property. To address this issue, we enforce Van Driest's scaling in the outer layer by modifying Eq. (1) as follows

$$\begin{aligned} y_T^+ \leq 50: &\quad d\bar{u}^+ = \mathscr{T}_{inner}^{-1} d\bar{U}_{inner}^+ + f_1^{-1} d\bar{U}_{wake}^+, \\ y_T^+ > 50: &\quad d\bar{u}^+ = f_1^{-1} d\bar{U}_{inner}^+ + f_1^{-1} d\bar{U}_{wake}^+, \end{aligned} \tag{8}$$

where $\mathscr{T}_{inner}$ denotes the inner-layer transformation kernel and y_T^+ is the transformed coordinate. The value of 50 is taken arbitrarily as a start of the logarithmic region.

REFERENCES

Bernardini, Matteo & Pirozzoli, Sergio 2011 Wall pressure fluctuations beneath supersonic turbulent boundary layers. *Physics of Fluids* **23** (8), 085102.

Bradshaw, Peter 1977 Compressible turbulent shear layers. *Annual Review of Fluid Mechanics* **9** (1), 33–52.

Cebeci, Tuncer & Smith, A. M. O. 1974 *Analysis of turbulent boundary layers*. Elsevier.

Ceci, Alessandro, Palumbo, Andrea, Larsson, Johan & Pirozzoli, Sergio 2022 Numerical tripping of high-speed turbulent boundary layers. *Theoretical and Computational Fluid Dynamics* **36** (6), 865–886.

Chauhan, Kapil, Nagib, Hassan & Monkewitz, Peter 2007 On the composite logarithmic profile in zero pressure gradient turbulent boundary layers. In *45th AIAA Aerospace Sciences Meeting and Exhibit*, p. 532.

Cogo, Michele, Salvadore, Francesco, Picano, Francesco & Bernardini, Matteo 2022 Direct numerical simulation of supersonic and hypersonic turbulent boundary layers at moderate-high Reynolds numbers and isothermal wall condition. *Journal of Fluid Mechanics* **945**, A30.

Coles, Donald 1956 The law of the wake in the turbulent boundary layer. *Journal of Fluid Mechanics* **1** (2), 191–226.

Coles, Donald 1962 The turbulent boundary layer in a compressible fluid. rand corp., rep. *Tech. Rep.*. R-403-PR.

Fernholz, HH & Finley, PJ 1980 A critical commentary on mean flow data for two-dimensional compressible turbulent boundary layers. *Tech. Rep.*. AGARD-AG-253.

Fernholz, HH & Finley, PJ 1996 The incompressible zero-pressure-gradient turbulent boundary layer: an assessment of the data. *Progress in Aerospace Sciences* **32** (4), 245–311.

Griffin, Kevin Patrick, Fu, Lin & Moin, Parviz 2021 Velocity transformation for compressible wall-bounded turbulent flows with and without heat transfer. *Proceedings of the National Academy of Sciences* **118** (34), e2111144118.

Hasan, Asif Manzoor, Larsson, Johan, Pirozzoli, Sergio & Pecnik, Rene 2023 Incorporating intrinsic compressibility effects in velocity transformations for wall-bounded turbulent flows. *Phys. Rev. Fluids* **8**, L112601.

Huang, Junji, Nicholson, Gary L, Duan, Lian, Choudhari, Meelan M & Bowersox, Rodney D 2020 Simulation and modeling of cold-wall hypersonic turbulent boundary layers on flat plate. In *AIAA Scitech 2020 Forum*, p. 0571.

Huang, PG, Bradshaw, P & Coakley, TJ 1993 Skin friction and velocity profile family for compressible turbulent boundary layers. *AIAA journal* **31** (9), 1600–1604.

Iyer, Prahladh S & Malik, Mujeeb R 2019 Analysis of the equilibrium wall model for high-speed turbulent flows. *Physical Review Fluids* **4** (7), 074604.

Jiménez, Javier, Hoyas, Sergio, Simens, Mark P & Mizuno, Yoshinori 2010 Turbulent boundary layers and channels at moderate Reynolds numbers. *Journal of Fluid Mechanics* **657**, 335–360.

Johnson, Dennis A & King, LS 1985 A mathematically simple turbulence closure model for attached and separated turbulent boundary layers. *AIAA journal* **23** (11), 1684–1692.

Kumar, Vedant & Larsson, Johan 2022 Modular method for es-

timation of velocity and temperature profiles in high-speed boundary layers. *AIAA Journal* **60** (9), 5165–5172.

Lee, Myoungkyu & Moser, Robert D 2015 Direct numerical simulation of turbulent channel flow up to $Re_\tau \approx 5200$. *Journal of Fluid Mechanics* **774**, 395–415.

Monkewitz, Peter A & Nagib, Hassan M 2023 The hunt for the Kármán 'constant' revisited. *Journal of Fluid Mechanics* **967**, A15.

Musker, AJ 1979 Explicit expression for the smooth wall velocity distribution in a turbulent boundary layer. *AIAA Journal* **17** (6), 655–657.

Nagib, Hassan M & Chauhan, Kapil A 2008 Variations of von Kármán coefficient in canonical flows. *Physics of fluids* **20** (10), 101518.

Nagib, Hassan M, Chauhan, Kapil A & Monkewitz, Peter A 2007 Approach to an asymptotic state for zero pressure gradient turbulent boundary layers. *Philosophical Transactions of the Royal Society A: Mathematical, Physical and Engineering Sciences* **365** (1852), 755–770.

Patel, A., Boersma, B. J. & Pecnik, R. 2016 The influence of near-wall density and viscosity gradients on turbulence in channel flows. *Journal of Fluid Mechanics* **809**, 793–820.

Pecnik, R & Hasan, Asif M 2023 Drag and heat transfer estimation. https://github.com/Fluid-Dynamics-Of-Energy-Systems-Team/DragandHeatTransferEstimation.git.

Pirozzoli, Sergio, Romero, Joshua, Fatica, Massimiliano, Verzicco, Roberto & Orlandi, Paolo 2021 One-point statistics for turbulent pipe flow up to $Re_\tau \approx 6000$. *Journal of Fluid Mechanics* **926**.

Schlatter, Philipp & Örlü, Ramis 2010 Assessment of direct numerical simulation data of turbulent boundary layers. *Journal of Fluid Mechanics* **659**, 116–126.

Schlatter, Philipp, Örlü, Ramis, Li, Qiang, Brethouwer, Geert, Fransson, Jens HM, Johansson, Arne V, Alfredsson, P Henrik & Henningson, Dan S 2009 Turbulent boundary layers up to $Re_\theta = 2500$ studied through simulation and experiment. *Physics of fluids* **21** (5), 051702.

Sillero, Juan A, Jiménez, Javier & Moser, Robert D 2013 One-point statistics for turbulent wall-bounded flows at Reynolds numbers up to $\delta^+ = 2000$. *Physics of Fluids* **25** (10), 105102.

Smits, Alexander J & Dussauge, Jean-Paul 2006 *Turbulent shear layers in supersonic flow*. Springer Science & Business Media.

Song, Yubin, Zhang, Peng, Liu, Yilang & Xia, Zhenhua 2022 Central mean temperature scaling in compressible turbulent channel flows with symmetric isothermal boundaries. *Physical Review Fluids* **7** (4), 044606.

Spalart, Philippe R 1988 Direct simulation of a turbulent boundary layer up to $R_\theta = 1410$. *Journal of Fluid Mechanics* **187**, 61–98.

Trettel, A. & Larsson, J. 2016 Mean velocity scaling for compressible wall turbulence with heat transfer. *Physics of Fluids* **28** (2), 026102.

Van Driest, Edward R 1951 Turbulent boundary layer in compressible fluids. *Journal of the Aeronautical Sciences* **18** (3), 145–160.

Van Driest, Edward R 1956*a* On turbulent flow near a wall. *Journal of the Aeronautical Sciences* **23** (11), 1007–1011.

Van Driest, Edward R 1956*b* *The problem of aerodynamic heating*. Institute of the Aeronautical Sciences.

Volpiani, Pedro S, Iyer, Prahladh S, Pirozzoli, Sergio & Larsson, Johan 2020 Data-driven compressibility transformation for turbulent wall layers. *Physical Review Fluids* **5** (5), 052602.

Wenzel, Christoph, Selent, Björn, Kloker, Markus & Rist, Ulrich 2018 DNS of compressible turbulent boundary layers and assessment of data/scaling-law quality. *Journal of Fluid Mechanics* **842**, 428–468.

Zagarola, Mark V & Smits, Alexander J 1998 A new mean velocity scaling for turbulent boundary layers. In *Proceedings of FEDSM*, , vol. 98, pp. 21–25.

Zhang, Chao, Duan, Lian & Choudhari, Meelan M 2018 Direct numerical simulation database for supersonic and hypersonic turbulent boundary layers. *AIAA Journal* **56** (11), 4297–4311.

Zhang, You-Sheng, Bi, Wei-Tao, Hussain, Fazle & She, Zhen-Su 2014 A generalized Reynolds analogy for compressible wall-bounded turbulent flows. *Journal of Fluid Mechanics* **739**, 392–420.